Stress and Loss of Adult Neurogenesis Differentially Reduce Hippocampal Volume

Supplemental Information

Chronic Unpredictable Restraint Stress

All unstressed rats were group-housed for the entire experiment. Stressed rats were restrained in clear, plexiglass tubes (Harvard Apparatus, Holliston, MA) in empty cages for an average of 6 hours a day for 4 weeks. Because rats habituate to restraint over time (1; 2), we modified standard chronic restraint protocols to maintain stress. Habituation is inhibited when stress is unpredictable (3; 4), so we randomly varied the onset (between 8am and 11am) and duration (5-7 hours) of restraint stress each day. We also changed the olfactory context cues in the stress environment daily (banana, peppermint, cinnamon, lemon, and vanilla; LorAnn Oils, Lansing, MI), which also minimizes habituation (5). In addition, we stressed under bright light during the normal dark phase of the cycle, which is more stressful than restraint during the light phase (6). Finally, because social housing can buffer the effects of stress (7; 8), we single-housed stressed rats during the 4-week stress period and thereafter. Non-stressed control rats in all stress experiments were pair housed throughout the experiment and were weighed daily then placed back into their cages.

Depressive-like Behavior Tests

Novelty-suppressed feeding (9) measures motivation to eat in a novel, potentially threatening environment. Rats were food deprived for 24 hours, and placed in a (40cm x 40cm) open arena with a pile of regular chow pellets in the center. The latencies to approach the food pellets and to begin eating food pellets were measured. Any rat that did not eat after 10 minutes of exploration was removed from the arena and assigned a latency of 10 minutes. After the test, the amount of food eaten in the rat's home cage during a 5-minute interval was measured to assess hunger in a safe context.

Sucrose preference (10) is a rat model for anhedonia that measures a rat's preference to drinking naturally preferable sweetened water compared to regular water. Rats were given a bottle of 1% sucrose water in addition to their regular water for a habituation period overnight. The next day, bottles were switched, and sucrose and water consumption levels were measured during a 10-minute testing interval.

MRI Volume Analysis

Rats were perfused transcardially with 4% paraformaldehyde containing 0.5% (v/v) Magnevist (Bayer Healthcare Pharmaceuticals, Lancaster, PA) to improve MRI contrast, and brains were left in the skulls and imaged while submerged in fixative to minimize distortion and interface artifacts. Ex-vivo MRI was performed using a Bruker 14.1T MR imaging spectrometer (Bruker Biospin, Billerica, MA) using a spoiled FLASH technique (12) with TR/TE=50/5.8 ms, and 1 signal averages. The resulting 3D images were acquired in 85 min with an acquisition resolution of 50 microns isotropic.

Scans were coded to conceal treatment group and analyzed using MIPAV (National Institutes of Health, Bethesda, MD). Using coronal slices, a 1:10 ratio of slices were analyzed for hippocampal volume starting at the same point for each brain (~11 slices total/brain). For each slice, dorsal and ventral areas within the dentate gyrus, CA3, and CA1 were traced, and volumes of each subfield as well as the entire hippocampus were estimated from these traces. Dorsal and ventral hippocampus were divided according to stereological coordinates (13; 14) with dorsal categorized as 0-4.5mm ventral from dura, and ventral categorized as >4.5mm ventral from dura.

Nissl Volume Analysis

Following MRI scanning, brains were dissected from the skulls and transferred to 10% glycerol/PBS for 24 hours and 20% glycerol/PBS for at least 48 hours. A 1:12 ratio of 40mm slices were cut coronally throughout the entire extent of the hippocampus (~11 slices analyzed total/brain) using a sliding microtome and transferred into PBS with 0.1% sodium azide. Slices

were mounted, counterstained with 0.5% Cresyl Violet (Sigma-Aldrich, St. Louis, MO), dehydrated in graded ethanol, cleared, and coverslipped under Permount.

Slides were coded to conceal treatment group and analyzed using an Olympus BX-51 brightfield microscope. Using StereoInvestigator (MBF Bioscience, Williston, VT), dorsal and ventral sections of the granule cell layer, hilar region, and molecular layer of the dentate gyrus, as well as the pyramidal cell layer, stratum oriens containing basal dendrites, and all layers containing pyramidal cell apical dendrites were traced. Area measurements of traces were analyzed in NeuroLucida Explorer to estimate volumes of layers, subfields, and the entire hippocampus.

Golgi Analysis

Rats were sacrificed via rapid decapitation and brains were quickly extracted, rinsed with dH_2O and immersed in a Golgi-Cox impregnation solution (Rapid GolgiStain kit; FD Neurotechnologies, Columbia, MD) for 3 weeks in the dark, then transferred to RapidGolgi Stain solution for 48-hours. 125mm sections were sliced coronally throughout the entire extent of the hippocampus using a sliding microtome, immediately mounted on Superfrost slides (ThermoFisher, Waltham, MA), and dried. For visualization, slides were rinsed 2x2minutes in dH_2O, incubated in RapidGolgi Stain developing solution for 10 minutes, rinsed 2x4minutes in dH_2O, dehydrated in 50%, 75%, 95%, and 4x100% ethanol for 4 minutes each, cleared with ClearAdvantage (PolySciences, Inc., Warrington, PA) 3x4minutes, and coverslipped with Permount.

Slides were coded to conceal treatment group prior to analysis. Six pyramidal cells each from the dorsal and ventral hippocampus of each brain were randomly chosen and traced in their entirety using an Olympus BX-51 brightfield microscope and Neurolucida software (MBF Bioscience, Williston, VT). For each brain, individual neuron measurements were averaged for each subregion and branching points, dendritic length, and Sholl analysis were determined, comparing conditions, using Neurolucida Explorer (MBF Bioscience, Williston, VT). Because

differential effects of stress on atrophy have been reported in short- and long-shaft neurons (11), we analyzed the classification of neurons analyzed in each brain and found equal proportions of each pyramidal neuron subtype in all treatment groups (Supplemental Figure S3A-B). These pyramidal neuron subtypes were therefore aggregated for further analysis.

Immunohistochemistry

To verify ablation of neurogenesis in TK rats (Supplemental Figure S1A,B) and to quantify stress-induced decreases in adult neurogenesis, slices were stained with the immature neuron marker, doublecortin (DCX). Series of sections (1:12) were immunostained with polyclonal goat anti-DCX (1:200; Santa Cruz, Dallas, TX; RRID: AB_2088494) and visualized with donkey anti-goat Alexa 488 fluorescent secondary (1:500; ThermoFisher, Waltham, MA; RRID: AB_2534102). Additional WT and TK hippocampal tissue was stained with GFAP to label astrocytes and isolectin IB4 (IB4) for labeling blood vessels. Free-floating sections were immunostained with polyclonal rabbit anti-GFAP (1:250; Agilent Technologies, Santa Clara, CA; RRID: AB_10013482), or biotinylated IB4 (1:100; Sigma-Aldrich, St. Louis, MO; RRID: AB_2313663) and visualized with donkey anti-rabbit Alexa 555 fluorescent secondary (1:500; ThermoFisher, Waltham, MA; RRID AB_162543) or Streptavidin Alexa 488 fluorescent secondary (1:1000; ThermoFisher, Waltham, MA; RRID AB_2336881).

Blood Vessel Analysis

Images from the dentate gyrus molecular layer were taken using a Zeiss confocal microscope (LSM 780; lasers: argon 458/488). Cross-sectional area covered by IB4 blood vessels was taken from 1mm optical sections, with all parameters optimized and held constant for background subtraction. Percent area covered by IB4 blood vessels was measured in five representative sections of the dentate gyrus and averaged for each brain.

Statistical Analysis

For single treatment experiments, 2x2 (treatment x volume-measurement technique) repeated-measures ANOVA were performed for each region of interest to compare volume-measuring techniques. Only rats that underwent MRI in Experiments 1-2 were used in these analyses. Individual t-tests for each measuring technique were conducted in addition, to determine whether significant shrinkage could be detected if either method had been used alone. All rats used for Nissl reconstruction (some of which were not imaged) were included in those tests. 2x2 (treatment x region) repeated-measures ANOVAs were performed to detect left/right hemisphere differences or dorsal/ventral differences for total hippocampus and subregions. For the combined stress and ablation volume data, 3x2 (condition x technique) repeated-measures ANOVAs were performed to compare volume-measuring techniques followed by Tukey post hoc tests if necessary. In addition one-way ANOVAs were performed for each measuring technique to determine if significant shrinkage could be detected by only performing one test. 3x2 (treatment x region) repeated-measures ANOVAs were performed to detect left/right hemisphere differences or dorsal/ventral differences for total hippocampus and subregions. For behavioral and Golgi analyses, 2x2 ANOVAs (genotype x stress) were run for behavior, branch points, and total dendritic length and 2x2x24 (genotype x stress x distance from soma) repeated-measures ANOVAs were run for Sholl analyses, followed by Newman-Keuls post hoc tests if necessary. To compare short- and long-shaft neuron effects, 2x2x2 (genotype x stress x shaft-type) repeated-measures ANOVAs were run.

Supplemental Table S1. 2x2 ANOVAs for dorsal-ventral and left-right volume analysis of 4 weeks of stress

	MRI					
Analysis	***Main Effect of Stress***		***Main Effect of Region***		***Interaction***	
	F(1,10)	***p***	**F(1,10)**	***p***	**F(1,10)**	***p***
HIP left/right	**10.66**	**.0085**	**5.01**	**.049**	0.16	.70
HIP dor/ven	**10.66**	**.0085**	2.92	.12	1.00	.34
DG dor/ven	**11.71**	**.0065**	**42.09**	**<.0001**	0.54	.48
CA3 dor/ven	2.32	.16	**83.26**	**<.0001**	3.37	.10
CA1 dor/ven	**9.26**	**.012**	**307.4**	**<.0001**	2.08	.18
	Nissl					
Analysis	***Main Effect of Stress***		***Main Effect of Region***		***Interaction***	
	F(1,18)	***p***	**F(1,18)**	***p***	**F(1,18)**	***p***
HIP dor/ven	**13.07**	**.002**	**39.79**	**<.0001**	0.91	.35
DG dor/ven	**10.91**	**.0039**	0.79	.39	2.90	.11
CA3 dor/ven	**6.16**	**.023**	1.19	.29	1.07	.31
CA1 dor/ven	**6.32**	**.022**	**132.2**	**<.0001**	<.01	.99

HIP, hippocampus: DG, dentate gyrus; **bold** = $p < .05$ result.

Supplemental Table S2. 2x2 ANOVAs for dorsal-ventral and left-right volume analysis of 4/16 weeks of VGCV treatment.

4 weeks VGCV MRI						
Analysis	***Main Effect of Genotype***		***Main Effect of Region***		***Interaction***	
	F(1,8)	***p***	**F(1,8)**	***p***	**F(1,8)**	***p***
HIP left/right	1.77	.22	**8.09**	**.022**	2.97	.12
HIP dor/ven	1.78	.22	**6.89**	**.03**	0.04	.84
DG dor/ven	**9.90**	**.013**	**207.4**	**<.0001**	0.25	.63
CA3 dor/ven	0.35	.57	**59.24**	**<.0001**	0.29	.60
CA1 dor/ven	0.04	.85	**65.88**	**<.0001**	0.36	.56
Nissl						
Analysis	***Main Effect of Genotype***		***Main Effect of Region***		***Interaction***	
	F(1,8)	***p***	**F(1,8)**	***p***	**F(1,8)**	***p***
HIP dor/ven	4.22	.074	**39.87**	**.0002**	1.92	.20
DG dor/ven	**9.57**	**.015**	**8.40**	**.02**	0.86	.38
CA3 dor/ven	0.95	.036	**5.61**	**.045**	0.30	.60
CA1 dor/ven	0.25	.63	**180**	**<.0001**	2.41	.16
16 weeks VGCV MRI						
Analysis	***Main Effect of Genotype***		***Main Effect of Region***		***Interaction***	
	F(1,6)	***p***	**F(1,6)**	***p***	**F(1,6)**	***p***
HIP left/right	**6.45**	**.044**	1.61	.25	1.59	.25
HIP dor/ven	**6.45**	**.044**	3.39	.12	0.23	.65
DG dor/ven	**6.24**	**.046**	**53.69**	**.0003**	0.44	.53
CA3 dor/ven	2.16	.19	**43.82**	**.0006**	3.59	.11
CA1 dor/ven	0.02	.90	**42.39**	**.0006**	0.03	.87
Nissl						
Analysis	***Main Effect of Genotype***		***Main Effect of Region***		***Interaction***	
	F(1,8)	***p***	**F(1,8)**	***p***	**F(1,8)**	***p***
HIP dor/ven	**8.38**	**.02**	**94.38**	**<.0001**	0.38	.55
DG dor/ven	**5.44**	**.048**	0.27	.62	1.51	.25
CA3 dor/ven	**7.84**	**.023**	2.43	.16	0.04	.85
CA1 dor/ven	1.14	.34	**50.01**	**.0001**	2.84	.13

HIP, hippocampus: DG, dentate gyrus; **bold** = $p < .05$ result.

Supplemental Table S3. 3x2 ANOVAs for dorsal-ventral and left-right volume analysis of 8 weeks of VGCV treatment plus 4 weeks of stress

	MRI						
Analysis	***Main Effect of Treatment***		***Main Effect of Region***		***Interaction***		***Significant Post-Hoc Tests***
	F(2,12)	***p***	**F(1,12)**	***p***	**F(2,12)**	***p***	
HIP left/right	**15.46**	**.0005**	**13.33**	**.003**	1.76	.21	WT vs TK and TK+stress
HIP dor/ven	**15.46**	**.0005**	**9.09**	**.01**	0.14	.87	WT vs TK and TK+stress
DG dor/ven	**17.79**	**.0003**	**51.36**	**<.0001**	0.06	.95	WT vs TK and TK+stress
CA3 dor/ven	**4.86**	**.028**	**194.1**	**<.0001**	2.76	.10	WT vs TK
CA1 dor/ven	**8.85**	**.004**	**98.92**	**<.0001**	0.32	.74	TK+stress vs WT and TK
	Nissl						
Analysis	***Main Effect of Treatment***		***Main Effect of Region***		***Interaction***		***Significant Post-Hoc Tests***
	F(2,12)	***p***	**F(1,12)**	***p***	**F(2,12)**	***p***	
HIP dor/ven	**5.15**	**.024**	**4.89**	**.047**	0.18	.84	WT vs TK and TK+stress
DG dor/ven	3.54	.062	**96.04**	**<.0001**	0.34	.72	WT vs TK
CA3 dor/ven	**4.22**	**.041**	**21.82**	**<.0001**	0.18	.84	WT vs TK
CA1 dor/ven	**6.15**	**.015**	**163**	**<.0001**	0.25	.78	TK+stress vs WT and TK

HIP, hippocampus: DG, dentate gyrus; **bold** = $p < .05$ result.

Supplemental Table S4. Layer volumes from Nissl-stained sections

Layer	Stress, 4 weeks		Inhibit NG, 4 weeks		Inhibit NG, 16 weeks		Inhibit NG, 8 weeks + stress		
	control	*stress*	*WT*	*TK*	*WT*	*TK*	*WT control*	*TK control*	*TK stress*
DG granule cell layer	7.27±0.67	**4.51±0.25***	5.68±0.86	4.84±0.26	5.26±0.28	5.07±0.92	6.62±0.68	6.55±0.98	6.33±0.59
DG hilus	5.08±0.32	4.60±0.28	4.71±0.25	4.23±0.24	4.52±0.06	4.08±0.39	5.09±0.89	4.49±0.14	5.26±0.44
DG molecular layer	18.06±1.15	**14.20±0.72***	16.03±0.63	**12.90±0.71***	16.66±0.80	**12.64±0.76***	17.06±0.97	**12.88±0.67***	14.52±0.71
CA3 pyramidal cell layer	6.34±0.44	**4.91±0.42***	5.62±0.65	4.90±0.79	4.85±0.11	4.56±0.57	5.51±0.22	**3.86±0.25***	**4.31±0.22***
CA3 apical (SL+SR+SLM)	10.73±0.48	9.76±0.48	10.20±0.47	8.93±0.55	10.30±0.27	9.45±0.44	11.11±0.35	**8.75±0.42***	10.27±0.69
CA3 basal (SO+Alveus)	7.22±0.83	6.54±0.36	7.51±1.27	6.47±1.05	8.41±0.35	**5.83±0.81**	7.65±0.21	**6.00±0.45***	**5.73±0.57***
CA1 pyramidal cell layer	5.40±0.35	4.88±0.35	4.13±0.29	4.13±0.16	4.20±0.15	4.27±0.19	3.85±0.19	3.57±0.12	**3.13±0.33***
CA1 apical (SR+SLM)	21.22±0.96	**18.69±0.66***	18.30±0.45	17.35±0.87	16.74±0.51	17.71±0.34	18.00±0.47	18.49±0.25	**15.81±0.68***
CA1 basal (SO+Alveus)	8.13±0.39	**7.03±0.27***	7.20±0.36	6.48±0.36	6.90±0.30	6.49±0.31	7.21±0.29	6.75±0.23	**5.88±0.33***

Values represent mean±SEM (mm^3); SL, stratum lucidum; SLM, stratum lacunosum-moleculare; SO, stratum oriens; SR, stratum radiatum; *, P<0.05 versus control, WT, or WT control.

Supplemental Table S5: Basal CA3 dendritic branching and length

	Dorsal				Ventral			
	WT control	*WT stress*	*TK control*	*TK stress*	*WT control*	*WT stress*	*TK control*	*TK stress*
Branch points	16.73±1.58	16.67±0.88	17.36±0.77	17.61±1.05	16.15±1.55	16.35±0.64	16.92±1.02	16.64±0.62
Length (μm)	1904.38±98.27	1777.62±74.91	1835.61±85.80	1790.28±91.58	1895.05±100.73	1931.49±83.96	1957.35±104.39	1885.16±54.30

Values represent mean±SEM; there were no significant differences

Supplemental Figures

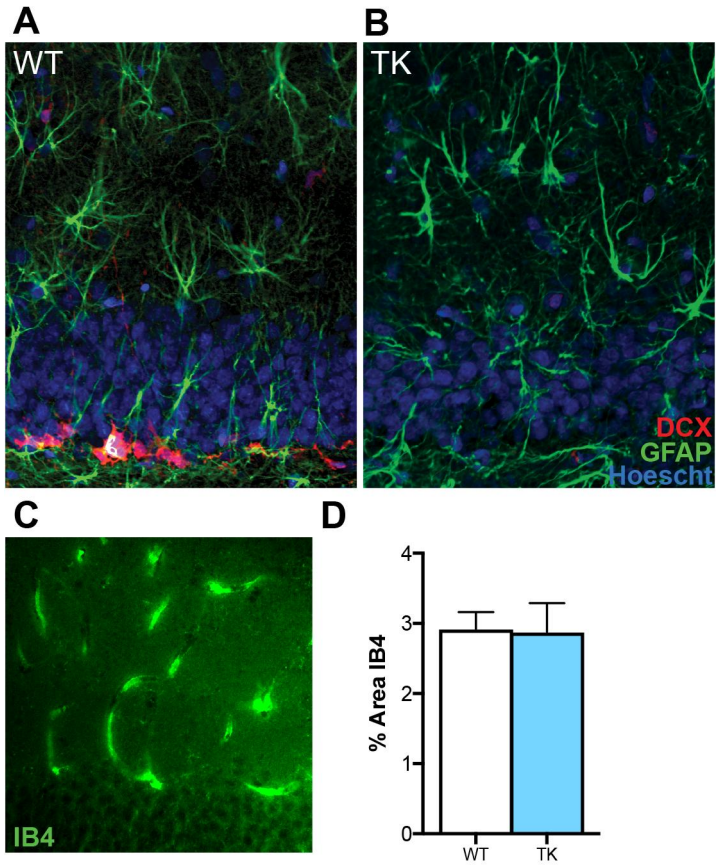

Supplemental Figure S1. Effect of VGCV on neurogenesis, astrocytes, and blood vessels in TK rats. ***A,B.*** TK rats (B) show no qualitative change in GFAP-astrocytes compared to WT rats (A); however TK rats show no expression of immature neuron marker, DCX. ***C.*** Representative photomicrograph of IB4, staining blood vessels in the dentate gyrus. ***D.*** WT and TK rats show similar coverage of the dentate gyrus with blood vessel ($t(10)$: 0.10, p = .92).

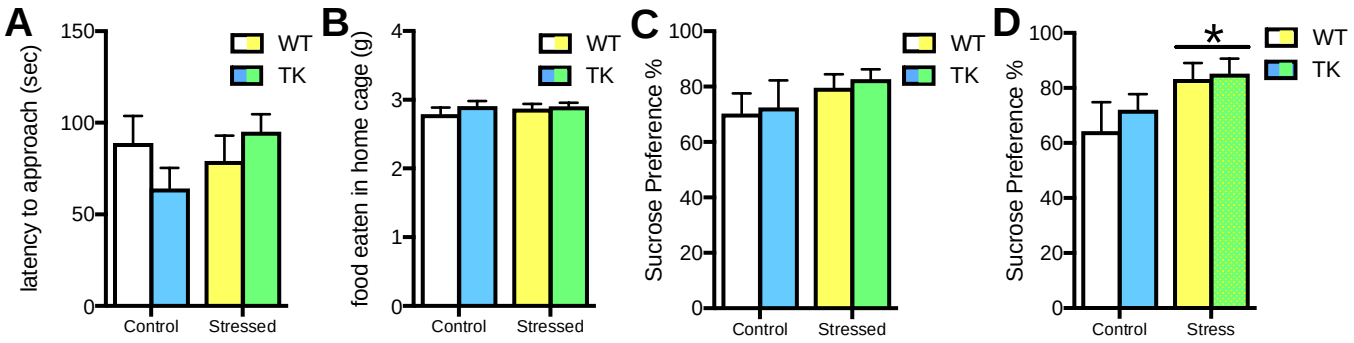

Supplemental Figure S2. Control data for depressive-like behavior tests. ***A.*** Chronic stress and inhibiting neurogenesis have no effect on the latency to approach food in the novelty-suppressed feeding test (2-way ANOVA, main effect of stress: $F_{(1,40)} = 0.72$, $p = .40$; main effect of genotype: $F_{(1,40)} = 0.13$, $p = .72$). ***B.*** All rats ate the same amount of chow in their home cage immediately after NSF testing (2-way ANOVA, main effect of stress: $F_{(1,40)} = 0.27$, $p = .60$; main effect of genotype: $F_{(1,40)} = 1.02$, $p = .32$; interaction: $F_{(1,40)} = 0.33$, $p = .57$). ***C.*** Sucrose preference was the same for all rats during habituation of sucrose (2-way ANOVA, main effect of stress: $F_{(1,29)} = 1.95$, $p = .17$; main effect of genotype: $F_{(1,29)} = 0.14$, $p = .71$; interaction: $F_{(1,29)} = 0.003$, $p = .95$). ***D.*** Stressed rats had higher sucrose preference during a 10-minute test (2-way ANOVA, main effect of stress: $F_{(1,31)} = 4.89$, $p = .035$).

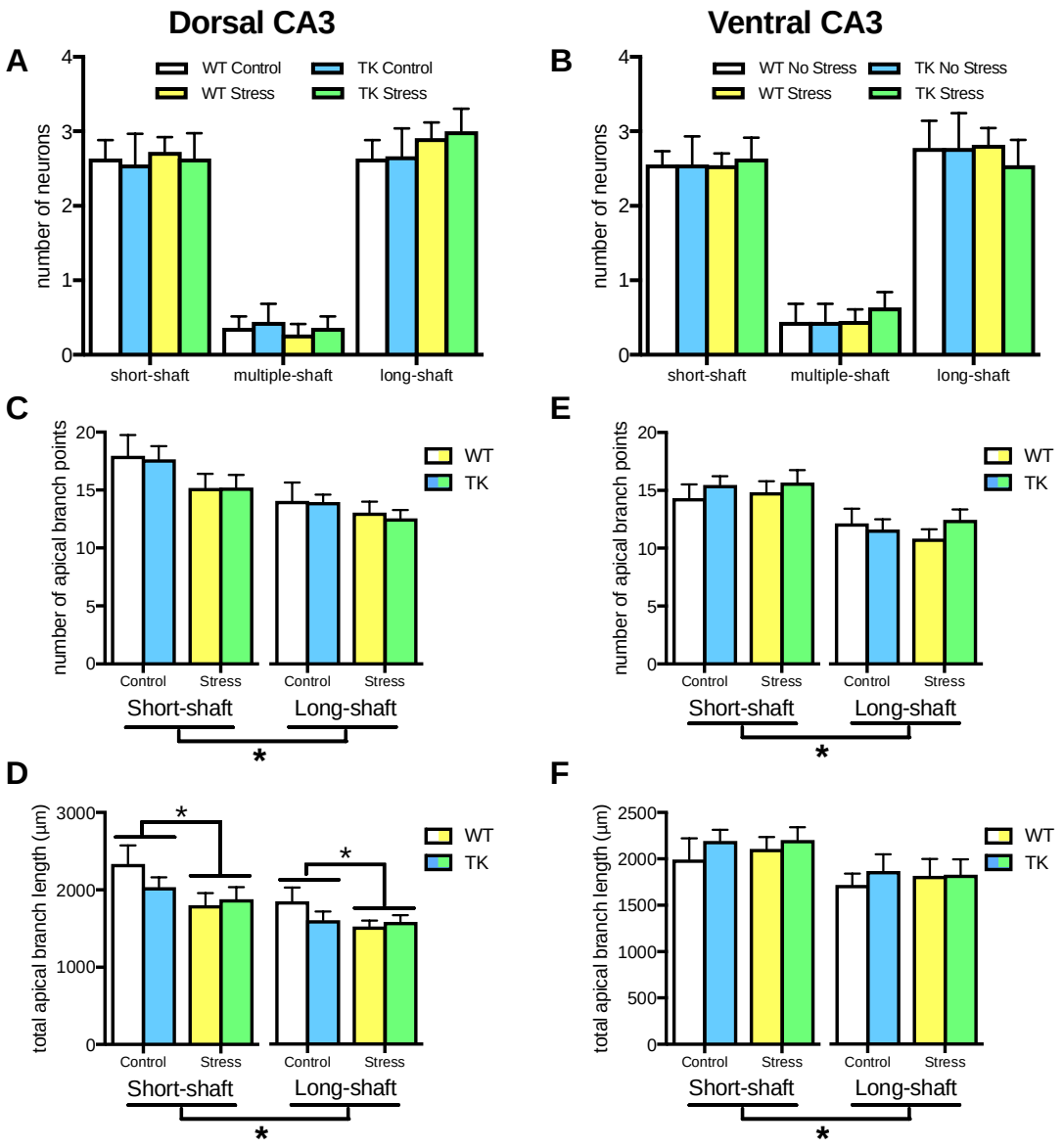

Supplemental Figure S3. Effects of stress and inhibition of neurogenesis on short- and long-shafted pyramidal neurons in CA3. ***A,B.*** The proportion of short-, long-, and multiple-shaft neurons analyzed was similar among all groups in dorsal (A) and ventral (B) CA3 (Dorsal long-shaft percentage: 2-way ANOVA: main effect of stress: $F_{(1,38)} = 0.37$, $p = .55$; main effect of genotype: $F_{(1,38)} = 0.01$, $p = .95$; interaction: $F_{(1,38)} = 0.02$, $p = .89$; Ventral long-shaft percentage: 2-way ANOVA: main effect of stress: $F_{(1,36)} = 0.06$, $p = .80$; main effect of genotype: $F_{(1,36)} = 0.27$, $p = .61$; interaction: $F_{(1,36)} = 0.20$, $p = .66$). ***C-F.*** Short-shaft neurons had more branch points and bigger dendritic trees than long-shaft neurons in both dorsal and ventral CA3 (3-way ANOVA: main effect of shaft: dorsal branch points: $F_{(1,36)} = 15.48$, $p = .0003$; ventral branch points: $F_{(1,36)} = 27.47$, $p < .0001$; dorsal length: $F_{(1,36)} = 12.65$, $p = .001$; ventral length: $F_{(1,36)} = 8.86$, $p = .005$), however both short- and long-shafted neurons showed the same stress effects on branch points and dendritic length (3-way ANOVA: main effect of stress: dorsal branch points: $F_{(1,36)} = 3.60$, $p = .06$; dorsal length: $F_{(1,36)} = 5.30$, * $p = .027$; shaft x stress interaction: dorsal branch points: $F_{(1,36)} = 0.78$, $p = .38$; ventral branch points: $F_{(1,36)} = 0.24$, $p = .63$; dorsal length: $F_{(1,36)} = 0.74$, $p = .40$; ventral length: $F_{(1,36)} = 0.02$, $p = .88$).

Supplemental References

1. Pitman DL, Ottenweller JE, Natelson BH (1988): Plasma corticosterone levels during repeated presentation of two intensities of restraint stress: chronic stress and habituation. *Physiology & Behavior*. 43: 47–55.

2. Babb JA, Masini CV, Day HEW, Campeau S (2014): Habituation of hypothalamic–pituitary–adrenocortical axis hormones to repeated homotypic stress and subsequent heterotypic stressor exposure in male and female rats. *Stress*. 17: 224–234.

3. Zhang W, Hetzel A, Shah B, Atchley D, Blume SR, Padival MA, Rosenkranz JA (2014): Greater Physiological and Behavioral Effects of Interrupted Stress Pattern Compared to Daily Restraint Stress in Rats. (L. B. M. Resstel, editor) *PLoS ONE*. 9: e102247–9.

4. Kearns RR, Spencer RL (2013): An unexpected increase in restraint duration alters the expression of stress response habituation. *Physiology & Behavior*. 122: 193–200.

5. Grissom N, Iyer V, Vining C, Bhatnagar S (2007): The physical context of previous stress exposure modifies hypothalamic–pituitary–adrenal responses to a subsequent homotypic stress. *Hormones and Behavior*. 51: 95–103.

6. Grissom N, Kerr W, Bhatnagar S (2008): Struggling behavior during restraint is regulated by stress experience. *Behavioural Brain Research*. 191: 219–226.

7. Weiss IC, Pryce CR, Jongen-Rêlo AL, Nanz-Bahr NI, Feldon J (2004): Effect of social isolation on stress-related behavioural and neuroendocrine state in the rat. *Behavioural Brain Research*. 152: 279–295.

8. Stranahan AM, Khalil D, Gould E (2006): Social isolation delays the positive effects of running on adult neurogenesis. *Nat Neurosci*. 9: 526–533.

9. Bodnoff SR, Suranyi-Cadotte B, Aitken DH (1988): The effects of chronic antidepressant treatment in an animal model of anxiety. *Psychopharmacology*. 95. doi: 10.1007/bf00181937.

10. Willner P, Towell A, Sampson D, Sophokleous S, Muscat R (1987): Reduction of sucrose preference by chronic unpredictable mild stress, and its restoration by a tricyclic antidepressant. *Psychopharmacology*. 93: 358–364.

11. Conrad CD, Ortiz JB, Judd JM (2016): Chronic stress and hippocampal dendritic complexity: Methodological and functional considerations. *Physiology & Behavior*. 1–16.

12. Haase A, Frahm J, Matthaei D, Hänicke W, Merboldt KD (2011): FLASH imaging: Rapid NMR imaging using low flip-angle pulses. *Journal of Magnetic Resonance*. 213: 533–541.

13. Banasr M, Soumier A, Hery M, Mocaër E, Daszuta A (2006): Agomelatine, a New Antidepressant, Induces Regional Changes in Hippocampal Neurogenesis. *Biological Psychiatry*. 59: 1087–1096.

14. Paxinos G (2004): *The Rat Brain in Stereotaxic Coordinates - The New Coronal Set*. Academic Press.